PHYSICAL REVIEW B VOLUME 61, NUMBER 22 1 JUNE 2000-II

Observation of individual Josephson vortices in $YBa_2Cu_3O_{7-\delta}$ bicrystal grain-boundary junctions

H. Xin,[1,2,3] D. E. Oates,[1,2] S. Sridhar,[4] G. Dresselhaus,[1,3], and M. S. Dresselhaus[1]
[1]*Department of Physics, Massachusetts Institute of Technology, Cambridge, Massachusetts 02139*
[2]*Lincoln Laboratory, Lexington, Massachusetts 02420*
[3]*AFRL, Hanscom AFB, Bedford, Massachusetts 01731*
[4]*Department of Physics, Northeastern University, Boston, Massachusetts 02115*
(Received 6 March 2000)

The response of $YBa_2Cu_3O_{7-\delta}$ bicrystal grain-boundary junctions to small dc magnetic fields (0–10 Oe) has been probed with a low-power microwave (rf) signal of 4.4 GHz in a microwave-resonator setup. Peaks in the microwave loss at certain dc magnetic fields are observed that result from individual Josephson vortices penetrating into the grain-boundary junctions under study. The system is modeled as a long Josephson junction described by the sine-Gordon equation with appropriate boundary conditions. Quantitative agreement between the experimental data and the model has been obtained. The hysteresis effect of dc magnetic field is also studied and the results of measurement and calculation are compared.

Grain-boundary junctions in high-temperature-superconducting (HTS) thin films have been studied extensively[1–9] due to their importance in both device applications and fundamental physics. The dynamics of Josephson vortices in Josephson junctions, which are analogous to the Abrikosov vortices in type-II superconductors,[10,11] is a very interesting subject, because of the mesoscopic physics involved. Much effort has been devoted to understanding the collective behavior of Josephson vortices in situations such as flux-flow devices.[12] The study of vortex physics on the mesoscopic scale has, in general, been hampered by the lack of suitable experimental probes.[13] It has also been known that for long junctions (junctions with a dimension longer than the Josephson penetration depth), Josephson vortices induced by the rf magnetic field cause nonlinear microwave losses which can severely limit the applicability of HTS materials in wireless communication applications.[6,14,15] Previous experiments and modeling have yielded qualitative agreement.[6,14] To further quantitatively understand the effect of the Josephson vortex dynamics on the microwave losses of HTS materials, it is important to study the influence of the Josephson vortices generated by dc magnetic fields. In this scenario, the vortex dynamics should be easier to probe, and an external dc magnetic field can emulate the physical situations of trapped flux or the earth's ambient magnetic field.

We report the observation of individual Josephson vortices generated by an external dc magnetic field and how these events affect microwave losses. We probe the Josephson vortex dynamics by using a small rf signal of 4.4 GHz in a microwave-resonator setup that includes a bicrystal grain-boundary junction. Each Josephson vortex entering the junction is manifested by a sharp peak in the microwave resistance, which is measured by our experimental setup. The second-order nonlinear sine-Gordon equation, which determines the dynamics of a long junction in the presence of dc and rf magnetic fields, is solved numerically. The measured and calculated results agree quantitatively as the dc field is increasing, and we are able to identify the series of sharp peaks observed in the microwave loss with the first several Josephson vortices penetrating into the grain-boundary junctions. Hysteresis effects upon decreasing the dc magnetic field have also been measured and calculated. Differences between calculated and measured losses in decreasing field will be discussed.

The junctions used in this study were fabricated from 140-nm-thick, epitaxial, *c*-axis-oriented, $YBa_2Cu_3O_{7-\delta}$ (YBCO) films deposited by laser ablation on 1 cm by 1 cm *r*-plane (1012) sapphire bicrystal substrates with a 24°-misorientation angle.[16] To characterize the microwave properties of the junction, we have used a microstrip-resonator configuration that allows us to distinguish the effects of the junction from those of the rest of the film. The resonator was patterned such that the junction is positioned at the midpoint of the microstrip, spanning the entire width of 150 μm, as shown in Fig. 1. The resonance frequency f_1 of the fundamental mode is 4.4 GHz with overtone resonant modes at $f_n \approx nf_1$ where n is an integer. At resonance, the fundamental mode is a half-wavelength standing wave with a current maximum at the midpoint of the resonator line, where the fabricated junction is positioned. In contrast, the $n=2$ mode is a full wavelength with a current node at the position of the junction. Therefore, by comparing the measured results of these two modes, we can separate the properties of the engineered grain-boundary junction from those of the remainder of the superconducting film. This resonator technique has previously been used to measure the microwave power-handling properties of the engineered junction in zero dc magnetic field.[6]

In this work, we have studied the characteristics of the junctions in small dc magnetic fields by injecting low-power rf input signals (pW) at the fundamental and the first overtone (4.4 and 8.7 GHz) of the resonator. The device was cooled in a magnetic field smaller than 0.01 Oe. The quality factor Q_0, which is proportional to the inverse of the microwave resistance, was measured for dc magnetic fields ranging from 0 to 10 Oe with a step size as small as 0.01 Oe, at temperatures ranging from 5 to 75 K. As expected, the measurements of the $n=2$ mode showed no observable dc magnetic-field dependence, since in this mode, the engineered junction does not contribute to the microwave loss,

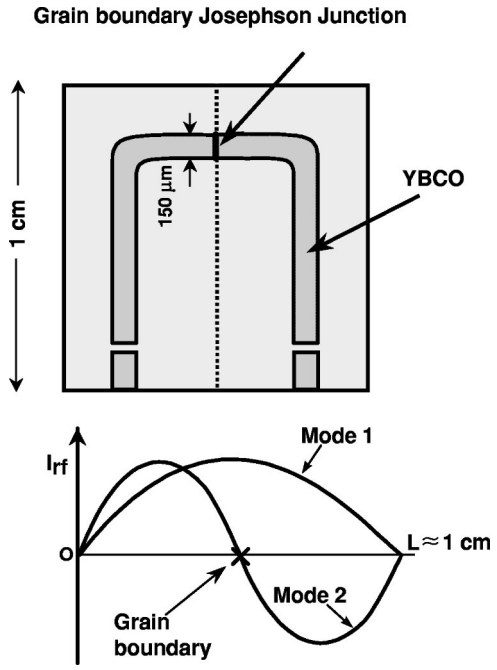

FIG. 1. The upper figure shows an engineered grain-boundary junction and the patterned YBCO microstrip resonator used in this study. The first ($n=1$, $f_1=4.4$ GHz) mode has a current peak at the junction, while the second mode ($n=2$, $f_2=8.7$ GHz) has a current node at the junction.

and the applied magnetic field H_{dc} is too small to affect the rest of the film. However, in the measurements of the $n=1$ mode, we observe an abrupt decrease in Q_0 at certain narrow ranges of dc magnetic fields, followed by a recovery to the zero-field value. This pattern is followed for all of the measured temperatures. Experimental data, plotted as $1/Q_0$ (proportional to the microwave resistance) versus dc magnetic field at various temperatures, are shown in Fig. 2. As described below, we interpret the observed peaks in $1/Q_0$ as single Josephson vortices penetrating into the junction. Furthermore, at each temperature, the data show a threshold field below which the microwave loss is low, and at which the first peak in the microwave loss is observed. The threshold field can be identified as the critical Josephson field H_{cJ}. Also, notice that the higher the temperature, the noisier the data become, indicating that thermal fluctuations may cause nucleation and annihilation of Josephson vortices. The noise is most apparent in the 75 K data. Two 24° junction samples have been measured and almost identical behavior was observed.

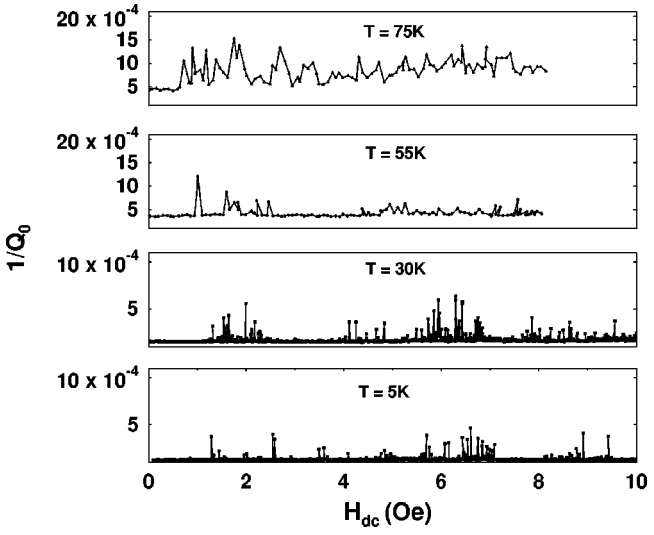

FIG. 2. Measured $1/Q_0$ of the microstrip resonator as a function of dc magnetic field at different temperatures. The threshold field at which the first peak in the microwave loss appears can be identified as the critical Josephson field H_{cJ}.

The length L of the grain-boundary junction is 150 μm, which is much greater than the Josephson penetration depth λ_J given by[17]

$$\lambda_J = \sqrt{\frac{\Phi_0}{2\pi\mu_0 J_c(2\lambda_L + d)}}, \tag{1}$$

where Φ_0 is the flux quantum, $\Phi_0 = h/2e = 2.07\times10^{-15}$ Wb, $\lambda_L \approx 0.2\,\mu$m is the London penetration depth of the film, and d is the physical grain-boundary interlayer thickness, which is negligible compared with λ_L. For a typical J_c of 10^2 to 10^4 A/cm^2, $\lambda_J \ll L$ and the long-junction regime applies.[17] For this situation, H_{cJ} is given by

$$H_{cJ} = 2\mu_0 J_c \lambda_J \propto \sqrt{J_c/\lambda_L}. \tag{2}$$

Above H_{cJ}, a Meissner state of the junction is not possible, and quantized flux in the form of Josephson vortices starts to penetrate into the junction from its edges.

The dynamics of a long-junction system are governed by the sine-Gordon equation,[18,19]

$$\lambda_J^2 \frac{\partial^2\phi(x,t)}{\partial x^2} = \sin\phi(x,t) + \tau_J \frac{\partial\phi}{\partial t}, \tag{3}$$

where $\phi(x,t)$ is the gauge-invariant phase difference of the superconducting wave function across the junction; $\tau_J = \Phi_0/2\pi d J_c \rho_n$, with ρ_n being the normal leakage resistivity of the junction. The capacitive term is omitted for our case of an overdamped junction.[6] We have solved Eq. (3) numerically with boundary conditions at the junction edges that include both the dc and microwave magnetic field. Similar treatments have been reported by other authors.[15,20] Thus,

$$\left.\frac{\partial\phi}{\partial x}\right|_{x=0,L} = \frac{2\pi(2\lambda_L + d)[H_{dc} \pm H_0 \sin(\omega t)]}{\Phi_0}, \tag{4}$$

where H_{dc} is the applied dc magnetic field, H_0 is the amplitude of the microwave magnetic field at the edges of the junction, and ω is the angular frequency of the microwave signal. The $\pm$ sign in Eq. (4) indicates that the directions of the microwave fields are opposite at the two edges of the junction. For this geometry, the microwave electric field is in the y direction which is defined to be normal to the junction area, and is given by

$$E_y(x,t) = \frac{\Phi_0}{2\pi d}\frac{\partial\phi(x,t)}{\partial t}. \tag{5}$$

The impedance and harmonic generation can then be calculated from the Fourier transform of the time-dependent electric field E_y,[15]

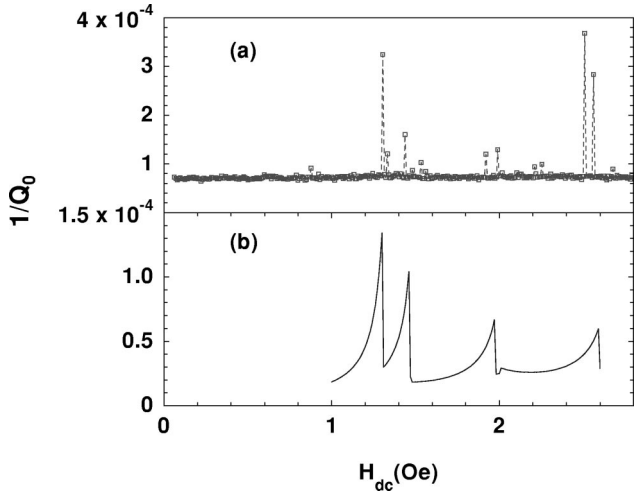

FIG. 3. (a) Measured $1/Q_0$ at 5 K vs increasing dc magnetic field compared with (b) the calculated effective Josephson-junction resistance vs dc magnetic field. The series of peaks observed are identified with individual Josephson vortices entering the junction.

$$R_n = \frac{2}{H_0}\int_0^{T_{\rm rf}} dt E_y(0,t)\sin(n\omega t), \tag{6}$$

$$X_n = \frac{2}{H_0}\int_0^{T_{\rm rf}} dt E_y(0,t)\cos(n\omega t), \tag{7}$$

where $T_{\rm rf}$ is the microwave period, n is a positive integer, R_1 and X_1 are proportional to the microwave resistance and reactance at the fundamental resonator frequency, and R_n and X_n for $n>1$ correspond to the nth harmonic generated in the junction. In Eqs. (6) and (7) we use only E_y at the edge of the junction, since the microwave loss is dominated by the behavior at the edges as found by Lehner *et al.*[14] The calculated resistance is compared with the measured results as a function of H_{dc} at $T=5$ K in Fig. 3. The parameters used in the calculation are $J_c = 4.078\times 10^2$ A/cm^2, $\rho_n = 6.75 \times 10^{-8}\,\Omega\,$cm^2, where ρ_n is obtained from dc I-V measurements, and J_c is taken to fit the experimentally observed H_{cJ} [Eq. (2)]. The calculation shows peaks in the microwave loss at the same dc magnetic fields as the experimental results.

We interpret the peaks in $1/Q_0$ as the result of Josephson vortices entering the junction. After zero-field cooling, the applied dc magnetic field is gradually increased and as long as $H_{dc}<H_{cJ}$, the external magnetic field is screened by the self-current in the junction (Meissner state). A further increase of the applied dc magnetic field so that $H_{dc}\approx H_{cJ}$ causes a Josephson vortex to almost enter the junction. Since the junction has two edges, this event is actually a two-vortex event, one from each edge. Because of the presence of the small rf magnetic field at the junction edges, two Josephson vortices are created and annihilated during each rf cycle. This state of the junction manifests itself in our experiment with sharply decreased Q_0 because the power dissipation is the highest when a Josephson vortex is created or annihilated at the edges.[14] With a slightly higher applied dc field, the Josephson vortex is driven completely into the junction and there is very little extra microwave loss once the vortex is in the junction.[14] As the applied field is increased further, the process is repeated each time another vortex enters the junction, until the junction is packed with Josephson vortices, and the collective properties of a large number of strongly interacting vortices have to be considered. Our numerical results are also qualitatively consistent with a previous linearized analytical treatment of the microwave absorption by a long junction in a magnetic field.[21]

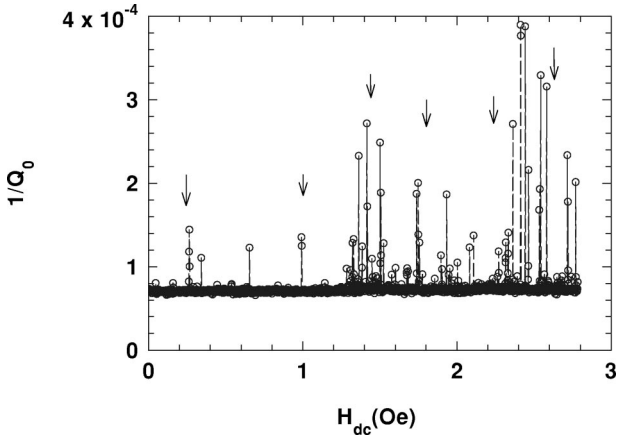

FIG. 4. Measured $1/Q_0$ at 5 K vs dc magnetic field (decreasing). The arrows in the figure indicate the calculated fields at which a quantized amount of flux leaves the junction.

The temperature dependence of H_{cJ} comes from that of J_c and λ_L in accordance with Eq. (2). The experimental temperature dependence of the onset of the first peak in the microwave resistance agrees roughly with the theoretically predicted $H_{cJ}(T)$.[18] This agreement is consistent with the hypothesis that the peaks observed in the microwave resistance of the grain-boundary junction are caused by single Josephson vortices entering the junction.

Since the calculation involving the rf magnetic field is computer-time consuming, we have also solved the static sine-Gordon equation without the perturbation from the rf signal. In order to get a physically meaningful solution, we keep the damping term $d\phi/dt$ in Eq. (3). After turning on the dc field at $t=0$, $\phi(x,t)$ is integrated in time until a static solution is reached. Magnetic-field and current distributions in the junction are then obtained. We have confirmed that the dc fields at which the microwave loss peaks appear correspond to the calculated dc fields at which individual Josephson vortices enter the junction. Therefore, results from the static dc calculation should provide sufficient information about the microwave losses.

We have calculated the hysteresis effects of the dc magnetic field using the static sine-Gordon solutions. To simulate our experiment, we have carried out the calculation with a dc field increasing from 0 to 3 Oe, then decreasing from 3 back to 0 Oe, with each step using $\phi(x)$ obtained from the previous step as the initial condition. The results show that as the dc field decreases, the Josephson vortices leave the junction at different field values than those at which vortices enter while the dc field is increasing. In addition, the number of expected microwave loss peaks (six) is more than in the case of the increasing field (four) because at some fields, one-half of a flux quantum leaves the junction, while all fluxon entry events cause a change of one flux quantum as the field increases. The measured $1/Q_0$ versus H_{dc} for decreasing H_{dc} is plotted in Fig. 4. The calculation-predicted dc fields at which

vortices leave the junction are indicated by the arrows in Fig. 4. Peaks of the microwave loss are observed but the agreement between the measured and the predicted results is not as good as the case of the increasing field. The calculations have considered only the case of a uniform junction. The good agreement with the experimental data for an increasing field indicates that the junction is sufficiently homogeneous for the assumption of uniform J_c to be a good approximation. The double-peak feature apparent in the measured data in Fig. 3 might be due to a slightly asymmetric J_c near the two edges of the junction so that there is one vortex penetrating into the junction from each edge at slightly different fields.

The nonuniform J_c and the pinning resulting from it might explain the differences seen in Fig. 4 between the calculated and measured behavior in decreasing field. In the case of increasing field, pinning is expected to have little effect on the process of vortex entry, and once in the junction, the losses are low, so the effects of pinning are not observed. On the other hand, pinning would affect the fields at which the vortices leave the junction by effectively adding to the potential barrier that a vortex must overcome to exit the junction. The pinning effects explain why the data for increasing field agree better with the calculation than the data for decreasing field. It will be interesting to consider defects in the junction in the calculation, so that the pinning of the Josephson vortices can be included.

The results of the measurements and calculations presented above show that we are able to probe individual Josephson vortices entering and exiting the bicrystal grain-boundary Josephson junctions under study. The microwave loss is not a monotonic function of external dc magnetic field and increases dramatically when a single vortex penetrates into or exits a long junction. Hysteretic behavior has been observed both in the experiments and the calculation. Since it is expected that HTS films contain weak links and the threshold field for vortex penetration can be very small, even the earth's ambient field or the field from trapped flux might have a significant impact on the microwave impedance of HTS films. In addition, the collective effects from many Josephson-junction-like weak links might also explain the anomalous dc response observed[22] in which R_S decreases with the application of a small magnetic field.

We gratefully acknowledge support for this work by the Air Force Office of Scientific Research. The authors wish to thank L. R. Vale and R. H. Ono at NIST, Boulder, CO for providing the samples used in this study, and J. Derov, G. Roberts, R. Webster, and J. Moulton at AFRL for their hospitality. We also wish to thank Dr. B. Willemsen for providing a rf probe used in this project.

[1] D. E. Oates, P. P. Nguyen, Y. M. Habib, G. Dresselhaus, M. S. Dresselhaus, G. Koren, and E. Polturak, Appl. Phys. Lett. **68**, 705 (1996).

[2] M. A. Hein, S. Beuven, M. Gottschlich, M. Perpeet, H. Piel, and M. Siegel, J. Supercond. **9**, 223 (1996).

[3] L. M. Xie, J. Wosik, and J. C. Wolfe, Phys. Rev. B **54**, 15 494 (1996).

[4] A. Cowie, L. F. Cohen, and M. W. Denhoff, Supercond. Sci. Technol. **12**, 431 (1999).

[5] H. Shimakage, J. C. Booth, L. R. Vale, and R. H. Ono, Supercond. Sci. Technol. **12**, 830 (1999).

[6] Y. M. Habib, C. J. Lehner, D. E. Oates, L. R. Vale, R. H. Ono, G. Dresselhaus, and M. S. Dresselhaus, Phys. Rev. B **57**, 13 833 (1998).

[7] Y. M. Habib, D. E. Oates, G. Dresselhaus, M. S. Dresselhaus, L. R. Vale, and R. H. Ono, Appl. Phys. Lett. **73**, 2200 (1998).

[8] P. P. Nguyen, D. E. Oates, G. Dresselhaus, and M. S. Dresselhaus, Phys. Rev. B **48**, 6400 (1993).

[9] R. G. Humphreys and J. A. Edwards, Physica C **210**, 42 (1993).

[10] I. O. Kulik, Zh. Éksp. Teor. Fiz. **51**, 1952 (1966) [Sov. Phys. JETP **24**, 1307 (1967)].

[11] A. M. Goldman and P. J. Kreisman, Phys. Rev. **164**, 544 (1967).

[12] Z. Y. Shen, *High-temperature Superconducting Microwave Circuits* (Artech House, Boston, 1994).

[13] C. A. Bolle, V. Aksyuk, F. Pardo, P. L. Gammel, E. Zeldov, E. Bucher, R. Boie, D. J. Bishop, and D. R. Nelson, Nature (London) **399**, 43 (1999).

[14] C. J. Lehner, D. E. Oates, Y. M. Habib, G. Dresselhaus, and M. S. Dresselhaus, J. Supercond. **12**, 2 (1999).

[15] J. Mcdonald and J. R. Clem, Phys. Rev. B **5**, 14 723 (1997).

[16] L. R. Vale, R. H. Ono, and D. A. Rudman, IEEE Trans. Appl. Supercond. **7**, 3193 (1996).

[17] M. Tinkham, *Introduction to Superconductivity* (McGraw-Hill, New York, 1996).

[18] A. Barone and G. Paterno, *Physics and Applications of the Josephson Effect* (Wiley, New York, 1982).

[19] A. M. Portis, J. Supercond. **5**, 319 (1992).

[20] Z. Zhai, P. V. Parimi, and S. Sridhar, Phys. Rev. B **59**, 9573 (1999).

[21] A. D. Golubov and A. E. Koshelev, Physica C **159**, 337 (1989).

[22] D. P. Choudhury, B. A. Willemsen, J. S. Derov, and S. Sridhar, IEEE Trans. Appl. Supercond. **7**, 1260 (1997).